The Journal of International Advanced Otology

J Int Adv Otol 2023; 19(4): 333–341 • DOI: 10.5152/iao.2023.22998

Original Article

Diffusion Tensor Imaging of Auditory Pathway: A Comparison of Pediatric Cochlear Implant Candidates and Healthy Cases

Direnç Özlem Aksoy, Yeşim Karagöz, Kemal Furkan Kaldırımoğlu, Melis Baykara Ulusan, Abdullah Soydan Mahmutoğlu

University of Health Sciences Istanbul Training and Research Hospital, Istanbul, Turkey

ORCID IDs of the authors: D.Ö.A. 0000-0001-8335-9673, Y.K. 0000-0002-1000-8271, K.F.K. 0000-0003-2712-7688, M.B.U. 0000-0002-4728-1802, A.S.M. 0000-0001-7987-0006.

Cite this article as: Aksoy DÖ, Karagöz Y, Kaldırımoğlu KF, Baykara Ulusan M, Mahmutoğlu AS. Diffusion tensor imaging of auditory pathway: A comparison of pediatric cochlear implant candidates and healthy cases. *J Int Adv Otol.* 2023;19(4):333-341.

BACKGROUND: We aimed to investigate the changes that may occur in the auditory neural network in pediatric congenital hearing loss cases.

METHODS: Fifty-four cochlear implant candidates and 47 normal-hearing controls were included in this retrospective study. Fractional anisotropy, radial diffusivity, and apparent diffusion coefficient maps were generated. We placed region of interest on the cochlear nucleus, superior olivary nucleus, lateral lemniscus, medial geniculate body, auditory radiation, Heschl's gyrus, inferior fronto-occipital fasciculus, superior longitudinal fascicle, and corpus callosum splenium. The area of the cochlear nerve was measured. Diffusion tensor imaging metrics, children's ages, and cochlear nerve area were compared.

RESULTS: Apparent diffusion coefficient and radial diffusivity values of patients were higher than the control group in all places except the radial diffusivity values of medial geniculate body. The fractional anisotropy values of the patients in lateral lemniscus, auditory radiation, Heschl's gyrus, inferior fronto-occipital fasciculus, superior longitudinal fascicle, and corpus callosum splenium were lower than the control group. There is a positive correlation between fractional anisotropy and age in both patient and control groups for all locations. The cochlear nerve area is lower in patients (0.88 ± 0.29) than in the control group (1.18 ± 0.14) ($P = .000$). The cochlear nerve area has a positive correlation with age in the patient group ($P = .000$) but has not in the control group. The cochlear nerve area positively correlates with fractional anisotropy values of all locations except fractional anisotropy values of medial geniculate body.

CONCLUSION: The alterations of diffusion tensor imaging metrics on the auditory pathway reflect the microstructural changes of white matter tracts.

KEYWORDS: Diffusion tensor imaging (DTI), pediatric hearing loss, auditory pathway, Fractional anisotropy (FA), radial diffusivity (RD), apparent diffusion coefficient (ADC).

INTRODUCTION

Hearing is a complex process that begins with the sound reaching the ear and continues with transmitting the stimulus to the auditory cortex. The first step is to transfer the sound to the neural pathway that starts with the organ of Corti in the cochlea. The stimulus in this neural network reaches the auditory cortex, passing through intermediate stations like the cochlear nucleus (CN), superior olivary nuclei (SON), lateral lemniscus (LL), and medial geniculate body (MGB).[1] Auditory stimulus is transmitted from the CN and SON by ipsilateral and crossing fibers. However, some neurons in the auditory system have crossing fibers at all levels of the auditory system. Because of this, the central auditory system receives information from both the ipsilateral and contralateral sides, with the dominance of the contralateral fibers.[2,3] Lin et al found lower fractional anisotropy (FA) values of the contralateral LL and higher radial diffusivity (RD) values in their diffusion tensor imaging (DTI) examination in patients with unilateral hearing loss. This supports the fact that the contralateral crossing fibers are dominant.[4] However, in another study

Corresponding author: Direnç Özlem Aksoy, e-mail: direncozlemaksoy@gmail.com

Received: November 23, 2023 • **Accepted:** February 27, 2023 • **Publication Date:** July 31, 2023

Available online at www.advancedotology.org

comparing with the hearing control group, FA values decreased in both ipsilateral and contralateral LL in cases with unilateral hearing loss. This also confirms that the central auditory pathway receives both ipsilateral and contralateral fibers.[5]

Sensorineural hearing loss (SNHL) is the most common cause of deafness. Any dysfunction of the auditory pathway, either the inner ear or central neural tract, can cause SNHL.[6] However, pathophysiological features of SNHL often cannot be identified, and most are accepted as idiopathic.[7] Computed tomography (CT) and magnetic resonance (MR) are the basic imaging modalities to reveal the anatomical and pathological causes of deafness. CT and MR provide useful information to evaluate temporal bone anatomy and congenital inner ear anomalies.[8] Magnetic resonance imaging (MRI) can reveal the anatomy of the internal acoustic canal and cochlear nerve and determine brain tumors and other pathologies that may affect the auditory pathways.[9]

Conventional imaging techniques cannot evaluate the central auditory network's functional integrity and microstructural pathophysiology.[10] DTI is an imaging modality that evaluates the white matter microstructural integrity of the central nervous system (CNS).

Axonal fiber extension and myelination in the auditory pathways depend on sound stimulation. These formations develop especially before 12 years old.[11,12] Therefore, congenital or early hearing loss may be expected to cause more changes in the microstructure of white matter pathways.[13] DTI provides a quantitative analysis of the magnitude and directionality of anisotropic diffusion to estimate the brain's white matter organization. The degree of anisotropy of water diffusion is higher parallel to the tract and affected by the deterioration of this structural integrity. So, diffusion metrics may show the location of the disruption in the auditory pathway. The apparent diffusion coefficient (ADC) is the amount of diffusion in a single direction and depends on diffusion anisotropy. In the anisotropic tissue, ADC is highest (diffusion is fastest) along the length of the pathway and is lower in other directions. Radial diffusivity represents the average of 2 shorter eigenvectors perpendicular to the diffusion's elementary direction. Radial diffusivity has been associated with axon, myelin, fiber density, and integrity, and increased RD indicates abnormalities.[14] Fractional anisotropy describes the direction-dependent amount of diffusion in a voxel and reflects the directional displacement of molecules.

Some studies have investigated DTI to explain the neuronal integrity of the auditory network in patients with hearing loss. Most of them were in adults and did not correlate the changes with the cochlear nerve.[4,5,10,15,16] We hypothesized that the microstructural changes might occur in the white matter due to hearing loss in children. Similarly, there may be a structural deterioration in the cochlear nerve, which might also be reflected in the calibers of the cochlear nerve. In this study, we aimed to investigate whether there are microstructural and functional changes in the auditory pathway that can be noticed via DTI metrics in pediatric cases with congenital SNHL and the correlation between these changes with cochlear nerve cross-sectional diameters and age.

MATERIAL AND METHODS

Subjects

We retrospectively reviewed the local PACS (Picture archiving and communication system) archive of the Istanbul Training and Research Hospital-Radiology department between January 2021 and June 2022 to find DTI MR examinations of children who were cochlear implant candidates and had bilateral hearing loss. After the elimination of patients who have inappropriate MRI images for measurement, 54 patients (23 girls and 31 boys; mean age 5.2 ± 4.3 years) under 18 years of age with bilateral severe to profound hearing loss (pure tone hearing test > 70 dB), who have DTI scans, were included in the study. The study did not include children with advanced inner ear anomalies with no cochlear nerve. Patients with known neurologic, neurocognitive, developmental, or behavioral deficits and pathologies in brain MR images have not enrolled in the study. Magnetic resonance imaging was performed under sedation on the subjects who could not complete the survey awake. The control group consisted of 47 age- and sex-matched children (15 girls and 32 boys; mean age 7.5 ± 4.3 years) under 18 years of age with normal hearing and normal brain images on MRI. Institutional review board approval was obtained for this retrospective study from the Clinical Researches Ethics Committee of the University of Health Sciences Istanbul Training and Research Hospital (Decision number: 2999). Written informed consent from the legal guardians of all children is contained in the hospital's medical records.

Image Acquisition

All participants have been imaged by a 1.5 T scanner (Siemens Healthcare, AeraMagnetom, Erlangen, Germany) equipped with a 16-channel head coil. The imaging protocol included axial T1-weighted (TR/TE: 500/9.9 ms; matrix: 256 × 125; NSA: 1; slice thickness: 3 mm), axial T2-weighted (TR/TE: 4.280/91 ms, matrix: 384 × 211, NSA: 1, slice thickness: 3 mm), axial fluid-attenuated inversion recovery (FLAIR) (TR/TE/TI: 8.000/118/23.687 ms; matrix: 256 × 140; NSA: 1; slice thickness: 3 mm), coronal FLAIR (TR/TE/TI: 8.000/118/23.695 ms, matrix: 256 × 144, NSA: 1, slice thickness: 3 mm), axial 3D constructive interference in steady state (CISS) T2 (TR/TE: 5.39/2.40 ms, matrix: 384 × 211, NSA: 1, slice thickness: 0.72 mm), and sagittal T2-weighted (TR/TE: 4.810/90; matrix: 320 × 247; NSA: 1; slice thickness: 5 mm) images. The DTI protocol included SE-EPI (spin-echo echo-planar imaging) images, TR = 6.000 ms, TE = 89 ms, 65 gradient directions, $b = 0$ s/mm^2 and $b = 1000$s/mm^2, 3-mm slice thickness, FOV (field of view) of 230 × 230 mm, and matrix: 128 × 128. This protocol is standard for brain MRI imaging at our institution.

Data Analysis

Diffusion tensor imaging images were transferred to the dedicated workstation (Syngo.Via, Erlangen, Germany). Fractional anisotropy, RD, and ADC maps were generated automatically. A free-hand region of interest (ROI) based technique was used utilizing the DTI data. The ROIs were placed on color-coded FA maps by 10 years of experienced neuroradiologists (YK) in all subjects. ROIs' placement and size were standardized bilaterally for each location. Depending on the location, the average size of ROI was between 10 and 15 mm^2. Correct placement of ROIs in the relevant anatomical area was ensured using reference T1- and T2-weighted images. Anatomical locations we examined were: CN, SON, LL, MGB, auditory radiation (AR), Heschl's gyrus (HG), inferior fronto-occipital fasciculus (IFOF),

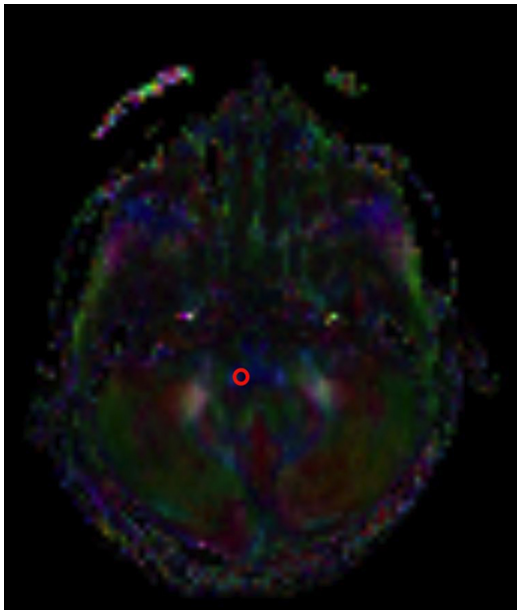

Figure 1. The region of interests on the cochlear nucleus (CN) on color-coded maps.

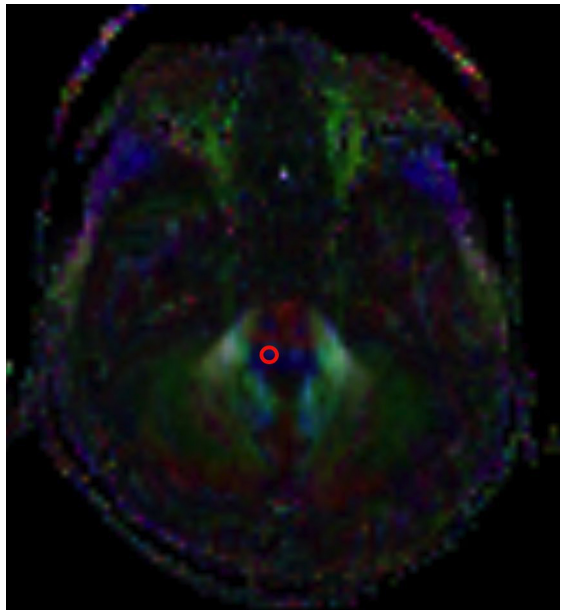

Figure 3. The region of interests on the lateral lemniscus (LL) on color-coded maps.

superior longitudinal fasciculus (SLF), and corpus callosum splenium (CCS) (Figures 1-9). We placed 1 ROI on the splenium of the corpus callosum and 2 ROIs bilaterally on other locations. Region of interest diameters placed symmetrically were adjusted to be almost identical to each other. We measured the cochlear nerve's cross-sectional area on the sagittal-oblique plane perpendicular to its long axis in the distal internal auditory canal on CISS images (Figures 10 and 11).

Statistical Analysis

Mean and standard deviation (SD) were used for descriptive statistics. The distribution of variables was checked with the Kolmogorov–Smirnov test. Independent samples *t*-test and Mann–Whitney *U*-test were used to compare quantitative data. The chi-square test was used for the comparison of qualitative data. Spearman correlation analysis was used in the correlation analysis. A $P \leq .05$ was considered statistically significant. All statistical analyses were performed using Statistical Package for the Social Sciences (SPSS) version 28.0 software for Windows (IBM SPSS Corp., Armonk, NY, USA).

RESULTS

Region of interest-based analysis of DTI metrics for the SNHL patient and control groups were compared. The mean values and the statistical analyses of FA, ADC, and RD for each auditory location (CN, SON, LL, MGB, AR, HG, IFOF, SLF, and CCS) are summarized in Table 1. ADC values are higher in the patient group, and the difference is statistically

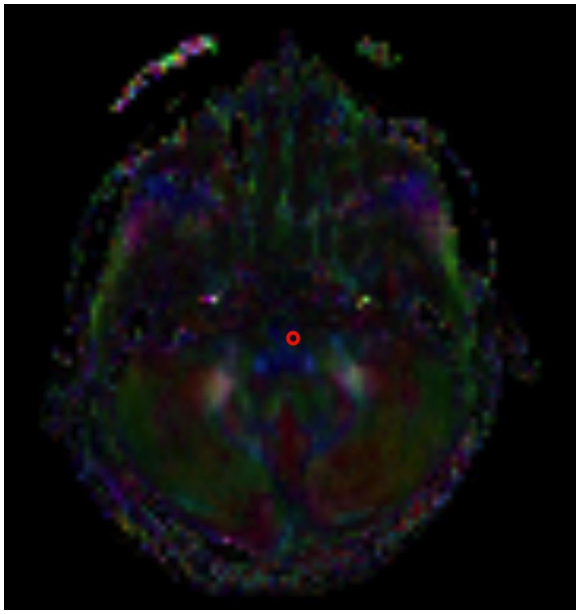

Figure 2. The region of interests on the superior olivary nucleus (SON) on color-coded maps.

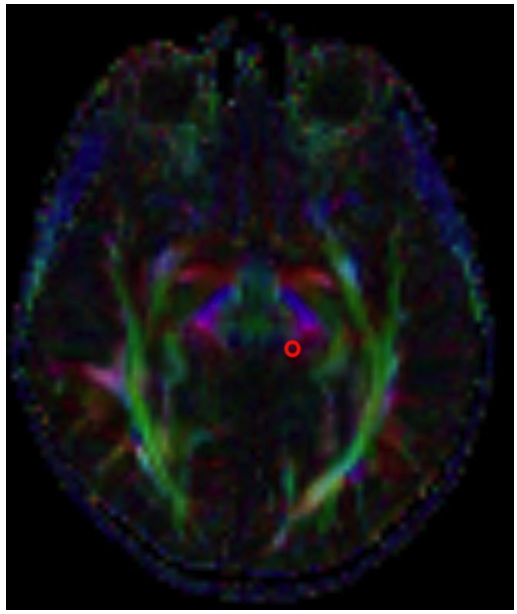

Figure 4. The region of interests on the medial geniculate body (MGB) on color-coded maps.

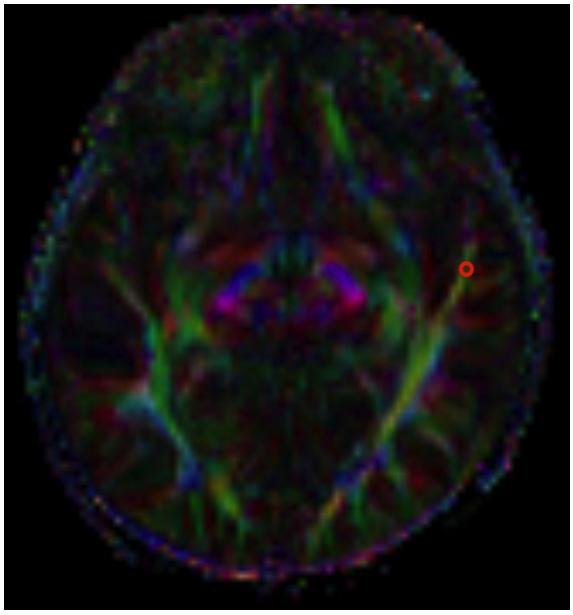

Figure 5. The region of interests on the auditory radiation (AR) on color-coded maps.

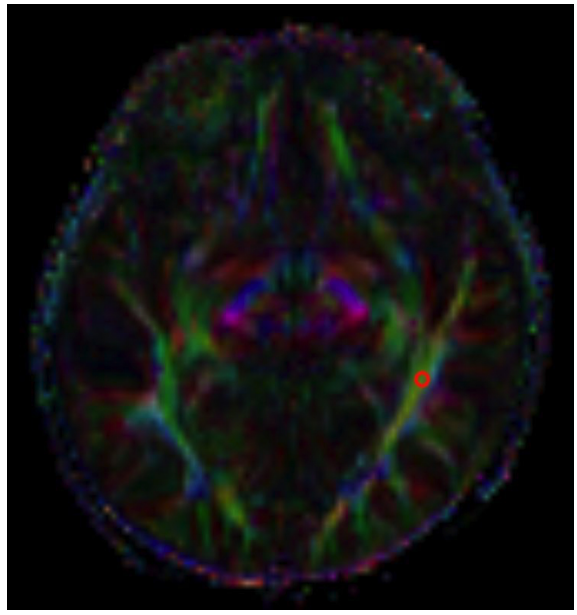

Figure 7. The region of interests on the inferior fronto-occipital fasciculus (IFOF) on color-coded maps.

significant between the patient and the control group in all places (Figure 12). Radial diffusivity values are higher in the patient group, and the difference is statistically significant between the patient and the control group in all places except MGB (Figure 13). The mean FA value of the patient group was found to be significantly lower in the patient group compared to the control at LL, AR, HG, IFOF, SLF, and CCS (Figure 14).

We evaluated correlations between the DTI metrics of each location and the ages of each group (Table 2). In both the patient and control groups, FA values of all locations were positively correlated with age. ADC and RD values of all locations were negatively correlated with age in the patient and the control groups.

The cochlear nerve cross-sectional area was lower in the patient group (0.88 ± 0.29) than in the control group (1.18 ± 0.14) ($P < .001$). The cochlear nerve area had a significantly positive correlation with age in the patient group ($P < .001$) but had no significant correlation in the control group. The cochlear nerve cross-sectional area has a positive correlation with FA values of all locations except FA values of MGB and a negative correlation with ADC and RD values (Table 3).

DISCUSSION

In DTI metrics, FA is considered a sensitive marker in demonstrating the white matter's axonal myelination and microstructural integrity.[17] Therefore, it has been reported that it can be used to evaluate neurodegenerative diseases that may disrupt the microstructural integrity

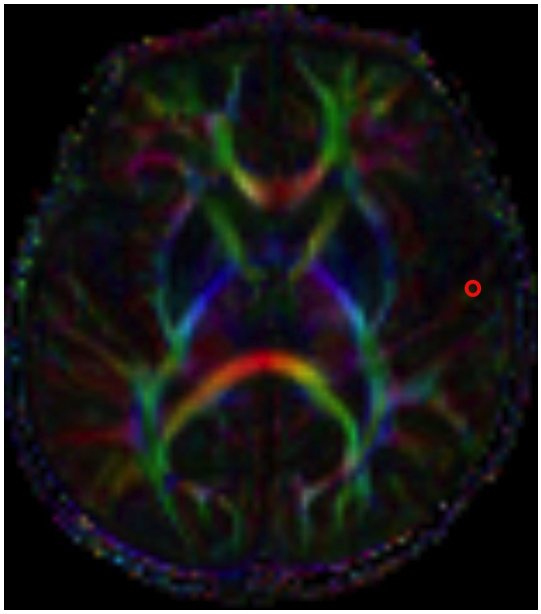

Figure 6. The region of interests on the Heschl's gyrus (HG) on color-coded maps.

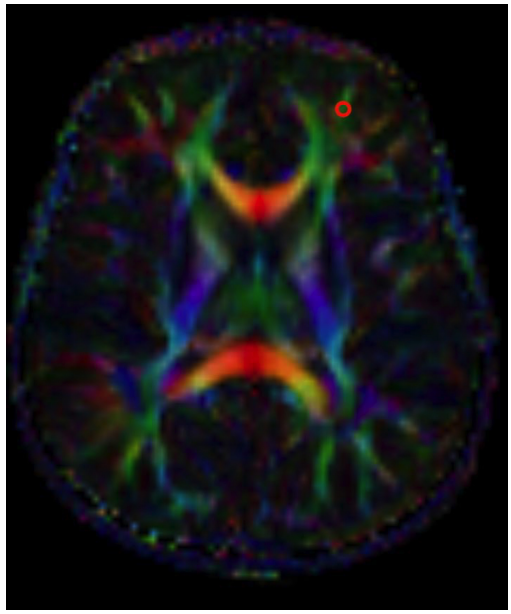

Figure 8. The region of interests on the superior longitudinal fascicle (SLF) on color-coded maps.

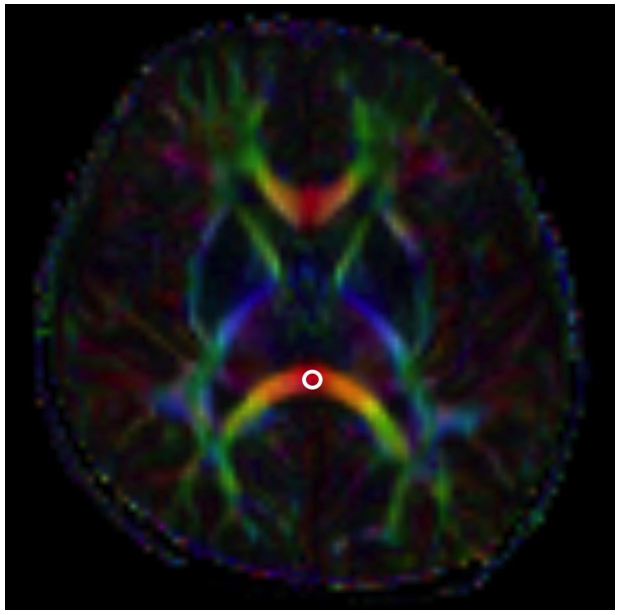

Figure 9. The region of interest on the corpus callosum splenium (CCS) on color-coded map.

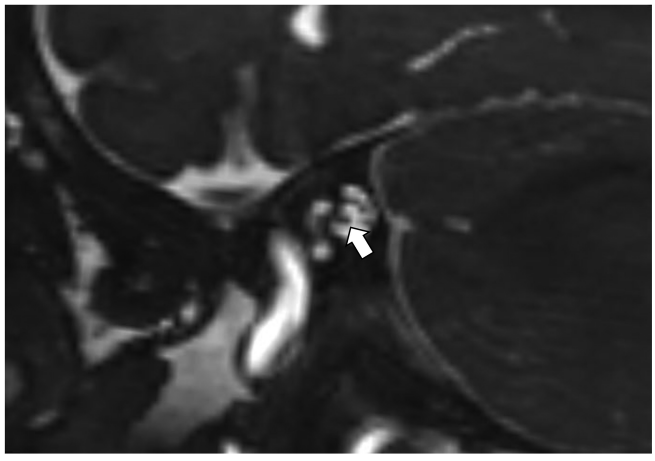

Figure 10. Cochlear nerve .

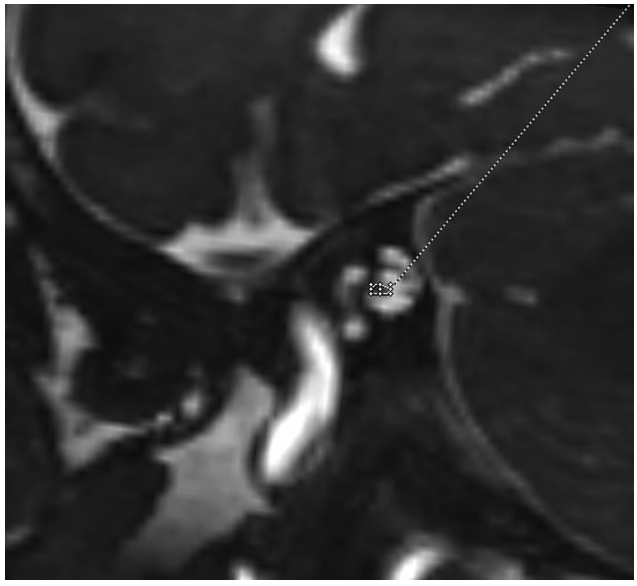

Figure 11. Cochlear nerve area measurement .

Table 1. Statistical Analysis of DTI Metrics and Cranial Nerve Area Measure

	Control Group	Case Group	*P*
	Mean ± SD	Mean ± SD	
CN			
ADC mean	826.3 ± 80.1	861.5 ± 71.1	***<.001***
FA mean	304.2 ± 53.7	299.0 ± 62.0	.528
RD mean	689.5 ± 80.9	712.8 ± 85.8	***.001***
SON			
ADC mean	844.7 ± 41.8	885.6 ± 68.6	***<.001***
FA mean	286.2 ± 61.4	272.6 ± 75.9	.168
RD mean	711.8 ± 57.9	754.2 ± 86.3	***<.001***
LL			
ADC mean	797.9 ± 48.3	834.5 ± 61.5	***<.001***
FA mean	533.7 ± 79.9	462.6 ± 105.4	***<.001***
RD mean	529.2 ± 80.9	598.0 ± 102.8	***<.001***
MGB			
ADC mean	818.4 ± 59.5	854.7 ± 108.5	***.001***
FA mean	300.2 ± 49.8	307.1 ± 57.7	.368
RD mean	689.6 ± 62.0	704.9 ± 88.3	.065
AR			
ADC mean	885.6 ± 85.0	918.3 ± 82.3	***.001***
FA mean	363.2 ± 75.2	319.0 ± 80.3	***<.001***
RD mean	705.3 ± 92.3	758.3 ± 101.2	***<.001***
HG			
ADC mean	908.1 ± 81.8	946.2 ± 81.2	***<.001***
FA mean	161.9 ± 43.7	141.4 ± 34.2	***<.001***
RD mean	833.1 ± 82.1	872.3 ± 96.5	***<.001***
IFOF			
ADC mean	895.5 ± 106.1	969.2 ± 114.3	***<.001***
FA mean	515.2 ± 67.7	481.6 ± 79.1	***.002***
RD mean	615.7 ± 89.1	683.6 ± 126.1	***<.001***
SLF			
ADC mean	821.3 ± 85.7	859.5 ± 78.4	***.001***
FA mean	476.3 ± 79.7	398.6 ± 79.6	***<.001***
RD mean	582.9 ± 94.5	661.0 ± 99.1	***<.001***
CCS			
ADC mean	910.2 ± 132.6	1038.9 ± 184.5	***<.001***
FA mean	751.0 ± 91.5	648.9 ± 107.9	***<.001***
RD mean	418.8 ± 157.0	599.1 ± 216.2	***<.001***
Cranial nerve area, mm^2	1.18 ± 0.14	0.88 ± 0.29	***<.001***

Statistically significant data with $P < .05$ are bolded.
ADC, apparent diffusion coefficient; AR, auditory radiation; CCS, corpus callosum splenium; CN, cochlear nucleus; DTI diffusion tensor imaging; FA, fractional anisotropy; HG, Heschl's gyrus; IFOF, inferior fronto-occipital fasciculus; LL, lateral lemniscus; MGB, medial geniculate body; RD, radial diffusivity; SLF, superior longitudinal fasciculus; SON, superior olivary nucleus.

of the CNS.[18] In cases with SNHL, a decrease in FA value was found, suggesting microstructural changes along the auditory pathway.[10,19] Reduced FA in different brain locations may indicate neural damage at different points in SNHL patients.[10] In our study, the FA values of

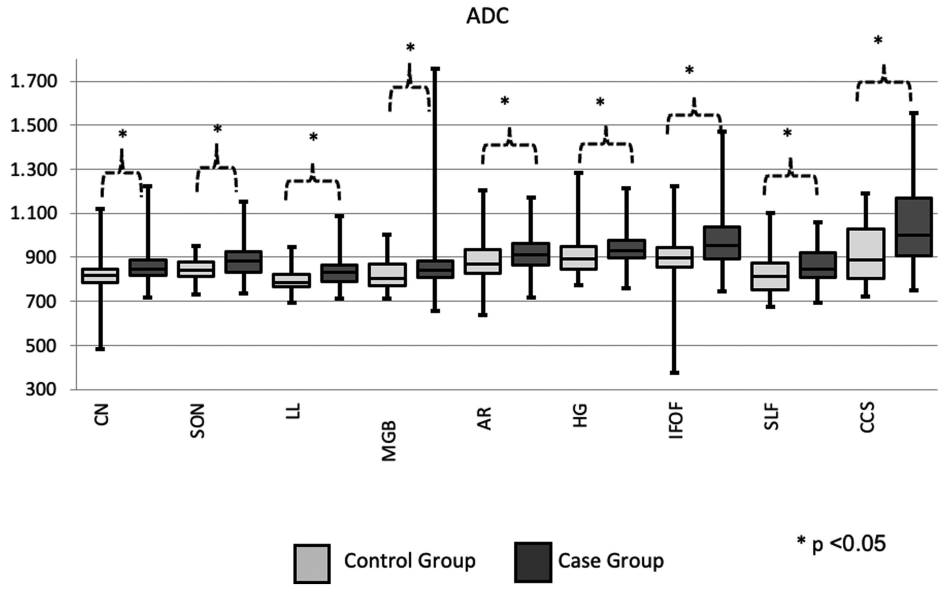

Figure 12. Comparative plot of ADC values between patient and control.

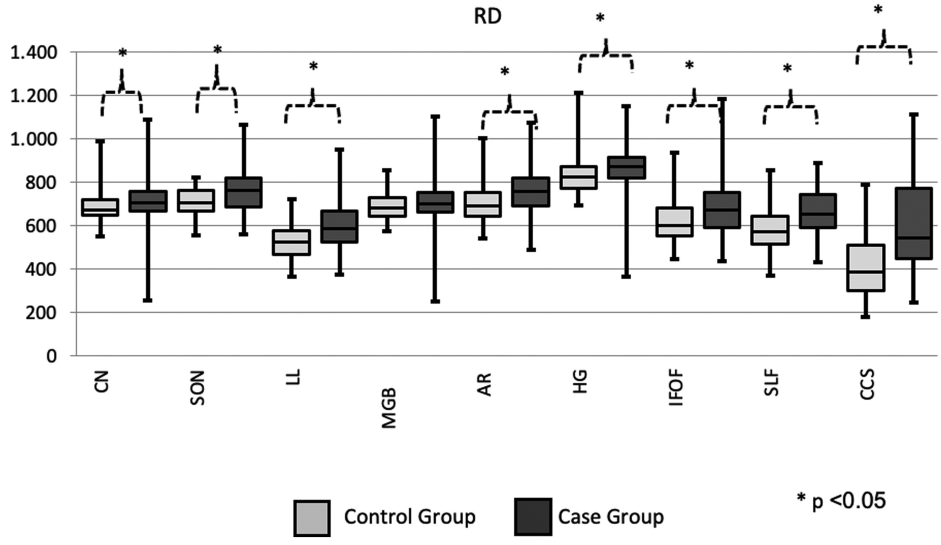

Figure 13. Comparative plot of RD values between patient and control.

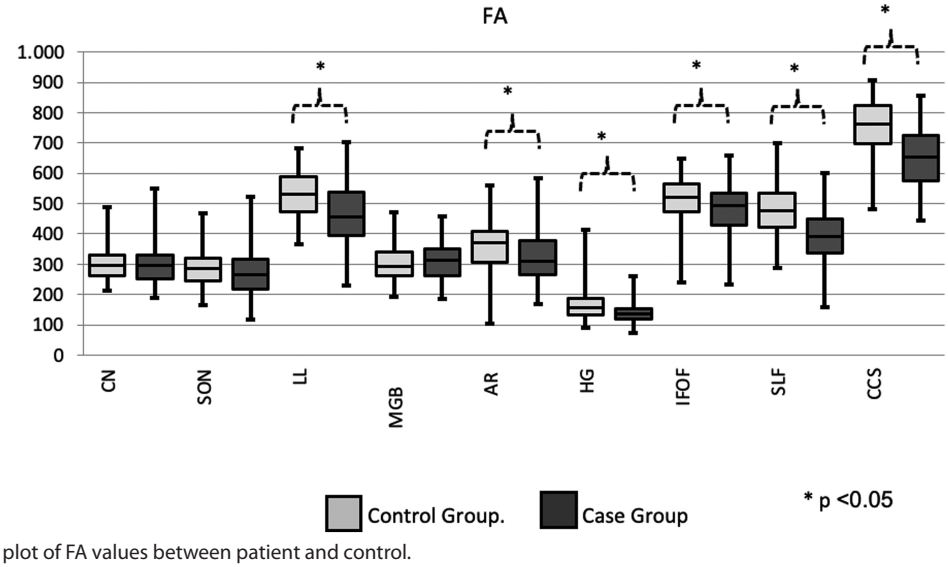

Figure 14. Comparative plot of FA values between patient and control.

Table 2. Correlation Analysis between Age and DTI Parameters

	Control Group		Case Group	
	r	*P*	*r*	*P*
CN ADC mean	−0.550	***<.001***	−0.522	***<.001***
CN FA mean	0.354	***<.001***	0.537	***<.001***
CN RD mean	−0.537	***<.001***	−0.680	***<.001***
SON ADC mean	−0.346	***.001***	−0.582	***<.001***
SON FA mean	0.422	***<.001***	0.592	***<.001***
SON RD mean	−0.413	***<.001***	−0.671	***<.001***
LL ADC mean	−0.584	***<.001***	−0.602	***<.001***
LL FA mean	0.552	***<.001***	0.589	***<.001***
LL RD mean	−0.599	***<.001***	−0.665	***<.001***
MGB ADC mean	−0.702	***<.001***	−0.623	***<.001***
MGB FA mean	0.344	***.001***	0.316	***.001***
MGB RD mean	−0.741	***<.001***	−0.606	***<.001***
AR ADC mean	−0.757	***<.001***	−0.809	***<.001***
AR FA mean	0.215	***.037***	0.627	***<.001***
AR RD mean	−0.668	***<.001***	−0.862	***<.001***
HG ADC mean	−0.704	***<.001***	−0.758	***<.001***
HG FA mean	0.304	***.003***	0.272	***.004***
HG RD mean	−0.676	***<.001***	−0.688	***<.001***
IFOF ADC mean	−0.550	***<.001***	−0.728	***<.001***
IFOF FA mean	0.505	***<.001***	0.669	***<.001***
IFOF RD mean	−0.594	***<.001***	−0.772	***<.001***
SLF ADC mean	−0.842	***<.001***	−0.780	***<.001***
SLF FA mean	0.332	***.001***	0.650	***<.001***
SLF RD mean	−0.690	***<.001***	−0.808	***<.001***
CCS ADC mean	−0.633	***<.001***	−0.631	***<.001***
CCS FA mean	0.560	***<.001***	0.414	***.002***
CCS RD mean	−0.612	***<.001***	−0.555	***<.001***

Statistically significant data with $P < .05$ are bolded.
ADC, apparent diffusion coefficient; AR, auditory radiation; CCS, corpus callosum splenium; CN, cochlear nucleus; DTI, diffusion tensor imaging; FA, fractional anisotropy; HG, Heschl's gyrus; IFOF, inferior fronto-occipital fasciculus; LL, lateral lemniscus; MGB, medial geniculate body; RD, radial diffusivity; SLF, superior longitudinal fasciculus; SON, superior olivary nucleus.

the patient group were lower than the control group, which was statistically significant at LL, AR, HG, IFOF, SLF, and CCS. In addition, we did not notice a statistically significant difference in FA values at CN, SON, and MGB. Wang et al[20] and Kim et al[21] did not find a significant difference in FA values at MGB. We concluded that inaccurate ROI locations would have caused these statistically insignificant results. As the exact locations of small anatomical nuclei can be difficult to identify accurately, ROI placements may not always be optimal. Lateral lemniscus, AR, HG, IFOF, SLF, and CCS are white matter tracts with a longitudinal orientation, which could be defined in multiple slices. This might provide more accurate ROI placement. Chang et al,[10] in their pilot study about DTI, claimed that the FA on the auditory pathway is lower in the patient group. The FA value in the LL and IC (inferior colliculus) of patients with SNHL was also decreased in Lin et al's[4] study compared to controls. Different studies compared RD and ADC values in addition to FA, as in our study. Wang et al[20] also compared RD by FA at different locations of the auditory pathway but found no significant difference between the patient and the control groups. There is an inversely proportional relation between FA and RD or ADC at different locations in our study. In locations where FA was low in the patient group, RD and ADC were high. Li et al[22] showed that auditory deprivation caused a decrease in FA values in the auditory cortex and corpus callosum and argued that this was mainly due to higher RD. RD is indicative of changes associated with myelination.[23] The increased RD may be due to myelin degeneration resulting from the decreased functional activity.[10] The decrease in FA was accompanied by an increase in RD, suggesting a dysmyelinating process. Fibers passing through the CCS show an extension to the bilateral temporal cortex. Decreased connectivity between the bilateral auditory cortices may cause reduced FA and increased RD in CCS. Kim et al[21] found low FA values of the auditory pathway but did not find a significant difference in ADC values in the patient group. On the contrary, we have found significantly higher ADC values in the patient group compared to the control group at all defined locations of the auditory pathway ($P < .05$). The increase in ADC has been reported to reflect edema, inflammation, deterioration of neural fiber integrity, and myelin or axonal integrity and may indicate microstructural changes in nerve fibers such as decreased FA.[24]

Bilateral moderate-to-profound hearing impairment is a common congenital disability with an incidence of 1-3 per 1000 newborns. The deprivation of hearing has a negative impact on language acquisition, school integration, and mental development. Numerous studies have proven the feasibility and effectiveness of hearing screening protocols. According to the Joint Committee on Infant Hearing (2007), all infants should be screened in the first month of age.[25] In acquiring speech functions after a cochlear implant, the relationship between auditory and speech centers is as well as auditory pathway function. The auditory pathway functions and their relations with the speech center should be adequately evaluated. The dorsal and ventral streams have been identified as essential for preserving the dynamic language network. The SLF is a part of the dorsal stream, and IFOF is a part of the ventral stream. The SLF establishes the temporal-parietal-frontal, and the IFOF establishes the occipital–temporal–frontal connections. The dorsal stream oversees auditory-motor integration, and the ventral stream manages speech recognition.[26] The FA, ADC, and RD values of patients in SLF and IFOF were statistically different from the control group in our study. Kim et al[15] found decreased FA values from the SLF and IFOF in patients, consistent with our results. Also, in the present study, we have found a statistically significant age-dependent increase of FA with an accompanying decrease of RD and ADC in both groups. In Park et al's[27] study, on the contrary, the correlations between age and FA values of SLF and IFOF were more robust in the DEAF(prelingually deaf children) group.

Researchers reported that the peak synaptic density in children with normal hearing is at 2-4 years. Dysfunctional synapses are reduced, reflecting the brain's customization of its functions to adapt to current conditions.[28] FA change of white matter tracts generally consists of 3 stages: rapid changes in the first year, slow changes in the second year, and relative stability after 24 months.[29] The age-related growth of white matter tracts may continue until 8 years in prelingually deaf children.[27] Our results were also consistent with these previous reports supporting the maturation of neural structure of auditory pathway with aging leading to reduced FA and concurrently

Table 3. Correlation Analysis between DTI Parameters and CN Area

	CN Area, mm²			CN Area, mm²	
	r	*P*		*r*	*P*
CN ADC MEAN	−0.271	***<.001***	HG ADC MEAN	−0.372	***<.001***
CN FA MEAN	0.239	***.001***	HG FA MEAN	0.252	***<.001***
CN RD MEAN	−0.300	***<.001***	HG RD MEAN	−0.375	***<.001***
SON ADC MEAN	−0.313	***<.001***	IFOF ADC MEAN	−0.403	***<.001***
SON FA MEAN	0.136	.054	IFOF FA MEAN	0.281	***<.001***
SON RD MEAN	−0.245	***<.001***	IFOF RD MEAN	−0.369	***<.001***
LL ADC MEAN	−0.291	***<.001***	SLF ADC MEAN	−0.346	***<.001***
LL FA MEAN	0.308	***<.001***	SLF FA MEAN	0.395	***<.001***
LL RD MEAN	−0.328	***<.001***	SLF RD MEAN	−0.424	***<.001***
MGB ADC MEAN	−0.267	***<.001***	CCS ADC MEAN	−0.364	***<.001***
MGB FA MEAN	0.089	.207	CCS FA MEAN	0.358	***<.001***
MGB RD MEAN	−0.226	***.001***	CCS RD MEAN	−0.373	***<.001***
AR ADC MEAN	−0.374	***<.001***			
AR FA MEAN	0.308	***<.001***			
AR RD MEAN	−0.397	***<.001***			

Statistically significant data with $P < .05$ are bolded.
ADC, apparent diffusion coefficient; AR, auditory radiation; CCS, corpus callosum splenium; CN, cochlear nucleus; DTI, diffusion tensor imaging; FA, fractional anisotropy; HG, Heschl's gyrus; IFOF, inferior fronto-occipital fasciculus; LL, lateral lemniscus; MGB, medial geniculate body; RD, radial diffusivity; SLF, superior longitudinal fasciculus; SON, superior olivary nucleus.

increased RD and ADC. Age-related microstructural changes occur in the elderly patient's central auditory system too. These changes are more pronounced in patients with presbycusis.[30] The leading cause of hearing loss in presbycusis cases is the peripheral (cochlear) component changes.[31] Some studies have shown that there are additional changes that DTI can detect in the central part of the auditory system in presbycusis cases.[31,32] However, it has been argued that the extent of hearing loss does not play an essential role in these changes.[31] There has yet to be a clear consensus on the results of these studies. While some studies did not detect significant changes in FA values in the auditory cortex, it was found in some studies.[30-32]

We found that the cochlear nerve cross-sectional area was lower in the patient group (0.88 ± 0.29) than in the control group (1.18 ± 0.14) ($P < .001$). Considering that the cochlear nerve cross-sectional area is also composed of axons, this finding is an expected result reflecting the thinning of non-stimulus-conducting pathways. The cochlear nerve cross-sectional area positively correlated with FA values in all locations other than SON and MGB.

There are some limitations in the current study. Our patient population is composed of cochlear implant candidates. Because most of them had profound hearing loss, we could not separate the SNHL patients according to the severity and the duration of hearing loss. We evaluated cases with bilateral hearing loss. Therefore, we could not compare the auditory pathways of both sides. The small and complex structures of the auditory pathway had potential pitfall for partial volume effects. Therefore, there are some difficulties in isolating structures with indistinct borders, such as the CN and MGB, from other important brainstem nuclei. Only 1 rater was responsible for determining the ROI. Using more than 1 rater would help evaluate the inter-rater reliability.

DTI is a method that can be used to reflect functional changes in the auditory pathway in patients with SNHL. Decreased FA values and increased ADC and RD values at different auditory pathway locations likely reflect the white matter microstructural changes in SNHL. The age-related changes in DTI parameters support the temporal maturation of white matter. Furthermore, the correlation of the cochlear nerve area with the DTI parameters indicates that axonal nerve degeneration also affects the cochlear nerve.

Ethics Committee Approval: Ethical committee approval was received from the Clinical Researches Ethics Committee of the University of Health Sciences Istanbul Training and Research Hospital (Approval No 2999).

Informed Consent: Written informed consent from the legal guardians of all children is contained in the hospital's medical records.

Peer-review: Externally peer-reviewed.

Author Contributions: Concept – D.Ö.A.,Y.K.; Design – D.Ö.A.,K.F.K.; Supervision – A.S.M.; Funding – N/A.; Materials – N/A.; Data Collection and/or Processing – Y.K.,K.F.K.; Analysis and/or Interpretation – Y.K.,M.B.U.; Literature Review – D.Ö.A.; Writing – D.Ö.A.; Critical Review – D.Ö.A.,Y.K.,A.S.M.

Declaration of Interests: The authors declare that they have no competing interest.

Funding: The authors declared that this study has received no financial support.

REFERENCES

1. Lee CC, Sherman SM. On the classification of pathways in the auditory midbrain, thalamus, and cortex. *Hear Res*. 2011;276(1-2):79-87. [CrossRef]

2. Peterson DC, Reddy V, Hamel RN. Neuroanatomy, auditory pathway. In: StatPearls. Treasure Island (FL): StatPearls Publishing. August 8, 2022.
3. Cope TE, Baguley DM, Griffiths TD. The functional anatomy of central auditory processing. *Pract Neurol*. 2015;15(4):302-308. [CrossRef]
4. Lin Y, Wang J, Wu C, Wai Y, Yu J, Ng S. Diffusion tensor imaging of the auditory pathway in sensorineural hearing loss: changes in radial diffusivity and diffusion anisotropy. *J Magn Reson Imaging*. 2008;28(3):598-603. [CrossRef]
5. Wu CM, Ng SH, Wang JJ, Liu TC. Diffusion tensor imaging of the subcortical auditory tract in subjects with congenital cochlear nerve deficiency. *AJNR Am J Neuroradiol*. 2009;30(9):1773-1777. [CrossRef]
6. Cunningham LL, Tucci DL. Hearing loss in adults. *N Engl J Med*. 2017;377(25):2465-2473. [CrossRef]
7. Baird SM, Nguyen K, Bhatia DDS, Wei BPC. Inner ear and retrocochlear pathology on magnetic resonance imaging for sudden and progressive asymmetrical sensorineural hearing loss. *ANZ J Surg*. 2019;89(6):738-742. [CrossRef]
8. Sennaroglu L, Saatci I. A new classification for cochleovestibular malformations. *Laryngoscope*. 2002;112(12):2230-2241. [CrossRef]
9. Glastonbury CM, Davidson HC, Harnsberger HR, Butler J, Kertesz TR, Shelton C. Imaging findings of cochlear nerve deficiency. *AJNR Am J Neuroradiol*. 2002;23(4):635-643.
10. Chang Y, Lee SH, Lee YJ, et al. Auditory neural pathway evaluation on sensorineural hearing loss using diffusion tensor imaging. *NeuroReport*. 2004;15(11):1699-1703. [CrossRef]
11. Rauschecker JP, Tian B. Mechanisms and streams for processing of "what" and "where" in auditory cortex. *Proc Natl Acad Sci U S A*. 2000;97(22):11800-11806. [CrossRef]
12. Zwolan TA, Ashbaugh CM, Alarfaj A, et al. Pediatric cochlear implant patient performance as a function of age at implantation. *Otol Neurotol*. 2004;25(2):112-120. [CrossRef]
13. Emmorey K, Allen JS, Bruss J, Schenker N, Damasio H. A morphometric analysis of auditory brain regions in congenitally deaf adults. *Proc Natl Acad Sci U S A*. 2003;100(17):10049-10054. [CrossRef]
14. Curran KM, Emsell L, Leemans A. Quantitative DTI measures. In: Van Hecke W., Emsell L., Sunaert S., eds. Diffusion Tensor Imaging. Springer, New York, NY; 2016. [CrossRef]
15. Kim DJ, Park SY, Kim J, Lee DH, Park HJ. Alterations of white matter diffusion anisotropy in early deafness. *NeuroReport*. 2009;20(11):1032-1036. [CrossRef]
16. Rykhlevskaia E, Gratton G, Fabiani M. Combining structural and functional neuroimaging data for studying brain connectivity: a review. *Psychophysiology*. 2008;45(2):173-187. [CrossRef]
17. Löbel U, Sedlacik J, Güllmar D, Kaiser WA, Reichenbach JR, Mentzel HJ. Diffusion tensor imaging: the normal evolution of ADC, RA, FA, and eigenvalues studied in multiple anatomical regions of the brain. *Neuroradiology*. 2009;51(4):253-263. [CrossRef]
18. Hasan KM, Gupta RK, Santos RM, Wolinsky JS, Narayana PA. Diffusion tensor fractional anisotropy of the normal-appearing seven segments of the corpus callosum in healthy adults and relapsing-remitting multiple sclerosis patients. *J Magn Reson Imaging*. 2005;21(6):735-743. [CrossRef]
19. Huang L, Zheng W, Wu C, et al. Diffusion tensor imaging of the auditory neural pathway for clinical outcome of cochlear implantation in pediatric congenital sensorineural hearing loss patients. *PLOS ONE*. 2015;10(10):e0140643. [CrossRef]
20. Wang H, Liang Y, Fan W, et al. DTI study on rehabilitation of the congenital deafness auditory pathway and speech center by cochlear implantation. *Eur Arch Otorhinolaryngol*. 2019;276(9):2411-2417. [CrossRef]
21. Kim S, Kwon HJ, Kang EJ, Kim DW. Diffusion-tensor tractography of the auditory neural pathway : clinical usefulness in patients with unilateral sensorineural hearing loss. *Clin Neuroradiol*. 2020;30(1):115-122. [CrossRef]
22. Li Y, Ding G, Booth JR, et al. Sensitive period for white-matter connectivity of superior temporal cortex in deaf people. *Hum Brain Mapp*. 2012;33(2):349-359. [CrossRef]
23. Song SK, Sun SW, Ramsbottom MJ, Chang C, Russell J, Cross AH. Dysmyelination revealed through MRI as increased radial (but unchanged axial) diffusion of water. *Neuroimage*. 2002;17(3):1429-1436. [CrossRef]
24. Yuan X, Li X, Xu Y, Zhong L, Yan Z, Chen Z. Microstructural changes of the vestibulocochlear nerve in patients with Ménière's disease using diffusion tensor imaging. *Front Neurol*. 2022;13:915826. [CrossRef]
25. Dimitriou A, Perisanidis C, Chalkiadakis V, Marangoudakis P, Tzagkaroulakis A, Nikolopoulos TP. The universal newborn hearing screening program in a public hospital: the importance of the day of examination. *Int J Pediatr Otorhinolaryngol*. 2016;91:90-93. [CrossRef]
26. Hickok G, Poeppel D. Dorsal and ventral streams: a framework for understanding aspects of the functional anatomy of language. *Cognition*. 2004;92(1-2):67-99. [CrossRef]
27. Park KH, Chung WH, Kwon H, Lee JM. Evaluation of cerebral white matter in prelingually deaf children using diffusion tensor imaging. *BioMed Res Int*. 2018;2018:6795397. [CrossRef]
28. Kral A, O'Donoghue GM. Profound deafness in childhood. *N Engl J Med*. 2010;363(15):1438-1450. [CrossRef]
29. Hermoye L, Saint-Martin C, Cosnard G, et al. Pediatric diffusion tensor imaging: normal database and observation of the white matter maturation in early childhood. *Neuroimage*. 2006;29(2):493-504. [CrossRef]
30. Peng L, Yu SL, Jing Y, Chen RC, Liang JP. Diffusion tensor imaging of the central auditory system in the elderly. *Lin Chung Er Bi Yan Hou Tou Jing Wai Ke Za Zhi*. 2016;30(8):637-640. [CrossRef]
31. Profant O, Škoch A, Balogová Z, Tintěra J, Hlinka J, Syka J. Diffusion tensor imaging and MR morphometry of the central auditory pathway and auditory cortex in aging. *Neuroscience*. 2014;260:87-97. [CrossRef]
32. Ma W, Li M, Gao F, et al. DTI analysis of presbycusis using voxel-based analysis. *AJNR Am J Neuroradiol*. 2016;37(11):2110-2114. [CrossRef]